SMAI 2021

A posteriori Finite-Volume local subcell correction of high-order discontinuous Galerkin schemes for the nonlinear shallow-water equations

Ali HAIDAR
Université de Montpellier 2, institut Montpelliérain Alexander Grotheindieck (IMAG)

21 juin 2021

Introduction

- The nonliear Shallow-Water (NSW) equations

$$\partial_t \eta + \partial_x q = 0, \tag{1a}$$

$$\partial_t q + \partial_x \left(uq + \frac{1}{2} g(\eta^2 - 2\,\eta\, b)\right) = -g\eta\partial_x b. \tag{1b}$$

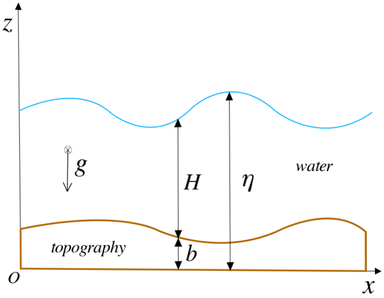

FIGURE – Free surface flow : main notations

Introduction

• Great efforts have been made since the sixties in order to produce accurate approximations of weak solutions of the NSW equations.

• large variety of numerical methods have been developed :

- **Finite-Volumes (FV) methods**
- Finite-Elements (FE) methods
- **Discontinuous Galerkin (DG)**
- spectral methods
- residual distribution methods

Introduction : DG methods (advantages)

High-order discontinuous Galerkin (**DG**) methods have become very popular to approximate the solutions of various linear and nonlinear partial differential equations.

- Combines the background of FE and FV methods
- Successfully validated in many domain of applications.
- Reach any Arbitrary high-order of accuracy in space.
- Handle complex geometries.
- Local conservation ; robustness ; strong stability properties.

Introduction : DG methods (disadvantages)

- DG still suffer from the lack of nonlinear stability. In particular, high-order DG methods may produce spurious oscillations in the presence of discontinuities or steeply varying gradients.
- DG may fails near wet/dry zones, negative water height in NSW.

Introduction : FV methods

- **FV advantages** : **(1)** Low computational cost, **(2)** their shock-capturing ability, which allows to preserve the discontinuous or steeply varying gradients, **(3)** and positivity preserving.
- **FV disadvantages** : Low accuracy, low order of convergence, solution dispersion.

Motivation : **FV** a very good choice for a **local** correction.

Plan du travail

1. Discrete formulation
   - DG formulation
   - DG formulation as a FV scheme on subcells
2. *A posteriori* local subcell correction
   - Admissibility criteria
   - Subcell low-order corrected FV fluxes
   - Well-balancing property
   - Preservation of the water height positivity
3. Numerical validation
   - Time marching algorithm
   - Test cases

Discrete formulation

Let $\Omega \subset \mathbb{R}$ denote the domain (a segment), such that $\Omega = \bigcup_i \omega_i$, where :

- $\omega_i = \left[x_{i-\frac{1}{2}}, x_{i+\frac{1}{2}}\right]$.
- h_{ω_i} is the length of element ω_i.
- $\mathbb{P}^k(\omega_i)$ the space of polynomials in ω_i.

Well-balanced DG scheme

$$\int_{\omega_i} \partial_t v_{h,i} \psi \mathrm{d}x = \int_{\omega_i} \mathrm{F}\left(v_{h,i}, b_{h,i}\right) \partial_x \psi \mathrm{d}x - [F\psi]_{i-1/2}^{i+1/2} + \int_{\omega_i} \mathrm{B}\left(v_{h,i}, b_{h,i}\right) \psi \mathrm{d}x, \quad \forall \psi \in \mathbb{P}^k(\omega_i). \tag{2}$$

$$F_{i+1/2} = F\left(v_{i+1/2}^-, v_{i+1/2}^+, b_{i+1/2}\right) \tag{3}$$

where $v_{i+1/2}^{\pm}$ and $b_{i+1/2} = b_{i+1/2}^{\pm}$ are the interpolated left and right values of ω_i interface $x_{i+1/2}$ and F is a consistent numerical flux.

DG formulation as a FV scheme on subcells

$$\partial_t \overline{v}_m^{\omega} = -\frac{1}{|S_m^{\omega}|}\left(\widehat{F}^{\,\omega}_{m+\frac{1}{2}} - \widehat{F}^{\,\omega}_{m-\frac{1}{2}}\right) + \overline{B}_m^{\omega}. \tag{4}$$

$$\widehat{F}^{\,\omega_i}_{m+\frac{1}{2}} = \mathrm{F}_{\omega_i}\left(\widetilde{x}^{\,\omega_i}_{m+\frac{1}{2}}\right) - C^{i-\frac{1}{2}}_{m+\frac{1}{2}}\left(\mathrm{F}_{\omega_i}(x_{i-\frac{1}{2}}) - F_{i-\frac{1}{2}}\right) - C^{i+\frac{1}{2}}_{m+\frac{1}{2}}\left(\mathrm{F}_{\omega_i}(x_{i+\frac{1}{2}}) - F_{i+\frac{1}{2}}\right) \tag{5}$$

we refer to [Haidar et al(2021)] and [Vilar(2019)] for more details.

Physical Admissibility Detection (PAD)

We define a sensor function that :

- Check if the sub-mean values $\overline{v}_m^{n+1}$ belongs to Θ.

$$\Theta = \left\{(H,q) \in^2;\ H \geq 0\right\}. \quad (6)$$

- Check if there is any *NaN* values.

Subcell Numerical Admissibility Detection (SubNAD)

In order to tackle the issue of spurious oscillations, we enforce a local *Discrete Maximum Principle*, at the subcell level, as follows :

- Check if, for $m = 1, \ldots, k+1$, the following inequalities hold :

$$\min\left(\overline{\eta}_{m-1}^{n}, \overline{\eta}_{m}^{n}, \overline{\eta}_{m+1}^{n}\right) \leq \overline{\eta}_{m}^{n+1} \leq \max\left(\overline{\eta}_{m-1}^{n}, \overline{\eta}_{m}^{n}, \overline{\eta}_{m+1}^{n}\right).$$

The SubNAD criterion relies on a DMP based on subcell mean values, and not the whole polynomial set of values.

Subcell low-order corrected FV fluxes

Replace the subcell mean value $\overline{v}_m^{n+1}$ by a new corrected one $\overline{v}_m^{\star,n+1}$, which is computed using a subcell first-order FV scheme of the form :

$$\overline{v}_m^{\star,n+1} = \overline{v}_m^n - \frac{\Delta t^n}{|S_m|}\left(F^l_{m+\frac{1}{2}} - F^r_{m-\frac{1}{2}}\right) + \Delta t^n \overline{B}_m, \tag{7}$$

where $F^l_{m+\frac{1}{2}}$, $F^r_{m-\frac{1}{2}}$ are some new subcell *first-order corrected* FV numerical fluxes .

Subcell low-order corrected FV fluxes

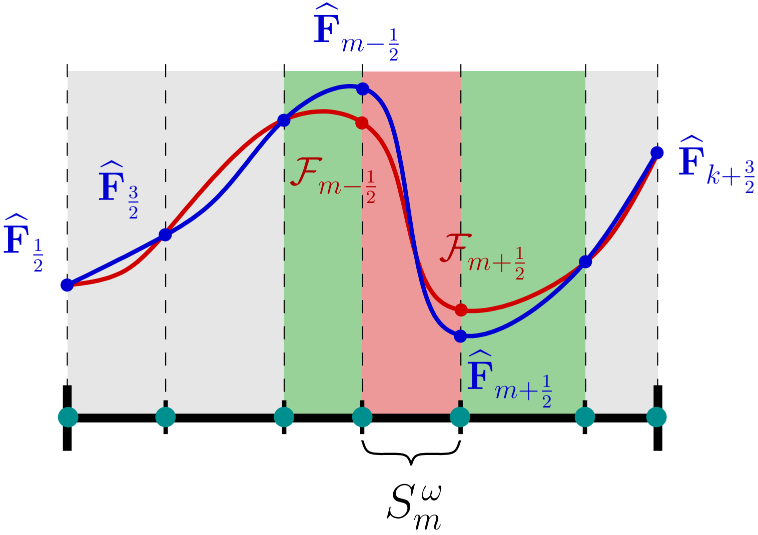

FIGURE – Sketch of the correction of the reconstructed fluxes at subcell boundaries

Subcell low-order corrected FV fluxes

$$\overline{v}_{m-1}^{\star,n+1} = \overline{v}_{m-1}^{n} - \frac{\Delta t^n}{|S_{m-1}|}\left(F^{l}_{m-\frac{1}{2}} - \widehat{\mathrm{F}}_{m-3/2}\right) + \Delta t^n \overline{B}_{m-1}, \quad (8)$$

$$\overline{v}_{m+1}^{\star,n+1} = \overline{v}_{m+1}^{n} - \frac{\Delta t^n}{|S_{m+1}|}\left(\widehat{\mathrm{F}}_{m+3/2} - F^{r}_{m+\frac{1}{2}}\right) + \Delta t^n \overline{B}_{m+1}. \quad (9)$$

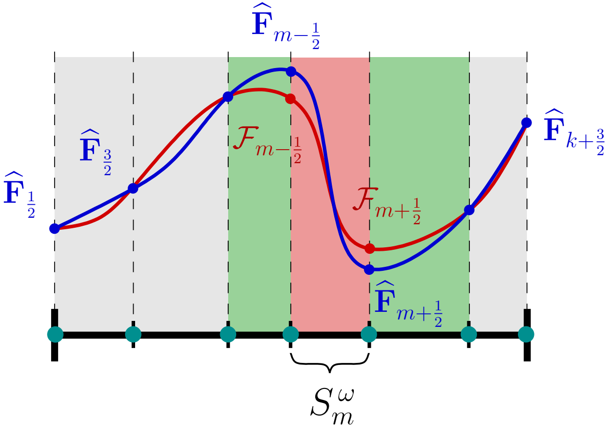

Subcell low-order corrected FV fluxes

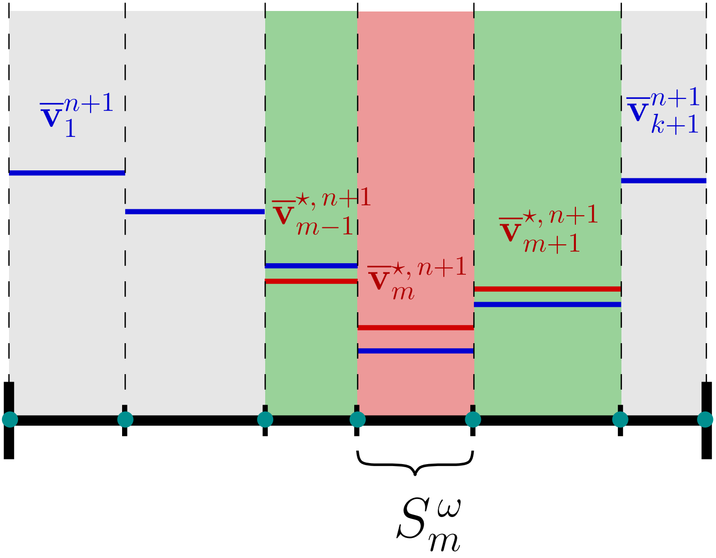

Well-balancing property (DG numerical flux)

We define the numerical flux function F on interface x as follows :

$$F = F(v^-_{i+1/2}, v^+_{i+1/2}, b_{i+1/2}), \tag{10}$$

where the numerical flux function is the global Lax-Friedrichs flux :

$$F(v^-, v^+, b) = \frac{1}{2}\left(\mathbf{F}(v^-, b) + \mathbf{F}(v^+, b) - \sigma(v^+ - v^-)\right), \tag{11}$$

with $\sigma = \max\limits_{\omega \in} \sigma_\omega$ and

$$\sigma_\omega = \max_m \left(|\overline{u}^\omega_m| + \sqrt{g\overline{H}^\omega_m} \right).$$

Well-balancing property (FV numerical flux)

We introduce some new Finite-Volume numerical fluxes on subcell's S_m left and right interfaces, denoted by $F^r_{m-\frac{1}{2}}$ and $F^l_{m+\frac{1}{2}}$, as follows :

$$F^l_{m+\frac{1}{2}} = F\left(\overline{v}^+_m, \overline{v}^-_{m+1}, \overline{b}^+_m\right) + \begin{pmatrix} 0 \\ g\overline{\eta}^+_m\left(\overline{b}^+_m - b_{\tilde{x}_{m+\frac{1}{2}}}\right) \end{pmatrix}, \quad (12)$$

$$F^r_{m-\frac{1}{2}} = F\left(\overline{v}^+_{m-1}, \overline{v}^-_m, \overline{b}^-_m\right) + \begin{pmatrix} 0 \\ g\overline{\eta}^-_m\left(\overline{b}^-_m - b_{\tilde{x}_{m-\frac{1}{2}}}\right) \end{pmatrix}. \quad (13)$$

Preservation of the water height positivity

$$\overline{v}_m^{\star,n+1} = \overline{v}_m^n - \frac{\Delta t^n}{|S_m|}\left(F^l_{m+\frac{1}{2}} - F^r_{m-\frac{1}{2}}\right) + \Delta t^n \overline{B}_m, \tag{14}$$

This scheme preserve positivity (on a sub-cell scale).

Remark

- Scheme (14) conserve height positivity. Actually we don't need more than that
- We have the well balancing for all schemes, on a sub-cell scale.

Time marching algorithm

We advance in time steps using the explicit SSP-RK schemes. For instance, writing the semi-discrete NSW equation in the operator form

$$\partial_t v_h + A_h(v_h) = 0,$$

we advance from time level n to $(n+1)$ with the third-order scheme as follows :

$$\begin{aligned} {v_h}^{n,1} &= {v_h}^n - \Delta t^n A_h({v_h}^n), \\ {v_h}^{n,2} &= \frac{1}{4}(3{v_h}^n + {v_h}^{n,1}) - \frac{1}{4}\Delta t^n A({v_h}^{n,1}), \\ {v_h}^{n+1} &= \frac{1}{3}({v_h}^n + 2{v_h}^{n,2}) - \frac{2}{3}\Delta t^n A_h({v_h}^{n,2}). \end{aligned}$$

Test cases : Smooth analytic solution

$$u_0(x) = \begin{cases} 1 & \text{if } x \leq 0, \\ e^{-x^{N_s+1}} & \text{elsewhere.} \end{cases}$$

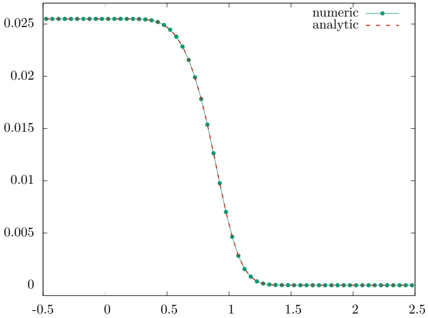

FIGURE – Test 1 - A new analytical solution for the NSW equations - Free surface elevation computed at $= 0.1\,s$ with the for $k = 3$ and $n_e = 60$.

Test cases : Smooth analytic solution

k	1		2		3	
h	$E^h_{L_2}$	$q^h_{L_2}$	$E^h_{L_2}$	$q^h_{L_2}$	$E^h_{L_2}$	$q^h_{L_2}$
$\frac{1}{15}$	5.91E-4	1.96	2.13E-5	3.19	3.20E-6	4.05
$\frac{1}{30}$	1.52E-4	2.02	2.33E-6	2.85	1.93E-7	4.18
$\frac{1}{60}$	3.73E-5	2.02	2.99E-7	2.95	1.06E-8	3.95
$\frac{1}{120}$	9.21E-6	-	4.18E-8	-	6.91E-10	-

TABLE – Test 1 - A new analytical solution for the NSW equations : L^2-errors between numerical and analytical solutions and convergence rates for η at time $t = 0.1s$

Test cases : discontinuity $t > t_c$

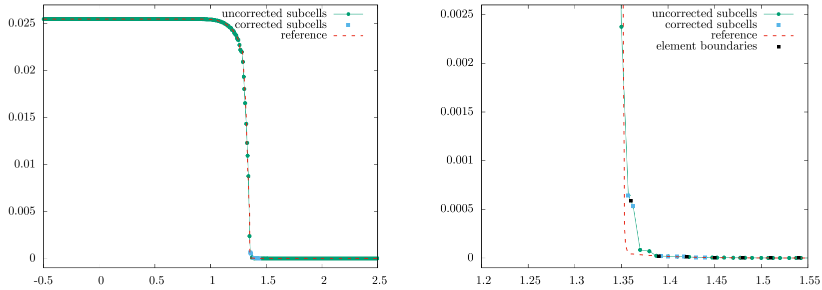

FIGURE – Test 1 - A new analytical solution for the NSW equations, with $k = 3$ and $n_e = 100$, with a zoom on the discontinuity and wet/dry interface.

Test cases : Dam-break (wet bottom)

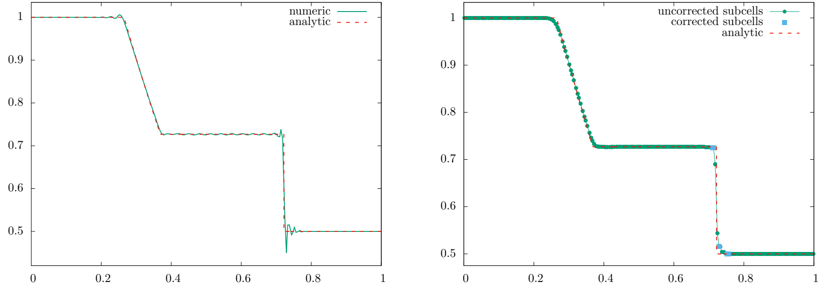

FIGURE – Test 2 - Dam break on a wet bottom, with $k = 3$ and $n_e = 50$ mesh elements.

Test cases : Dam-break (wet bottom)

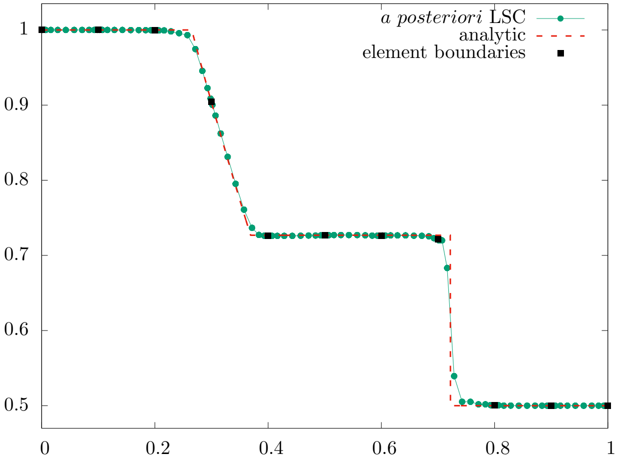

FIGURE – Test 2 - Dam break on a wet bottom, with $k = 9$ and $n_e = 10$.

Well-balancing property

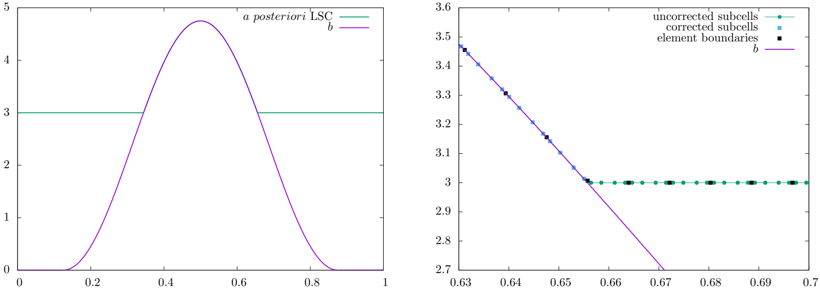

FIGURE – Test 3 - Preservation of a motionless steady state - Free surface elevation at $= 50s$ (left), with a zoom on the wet/dry interface (right).

Carrier and Greenspan periodic

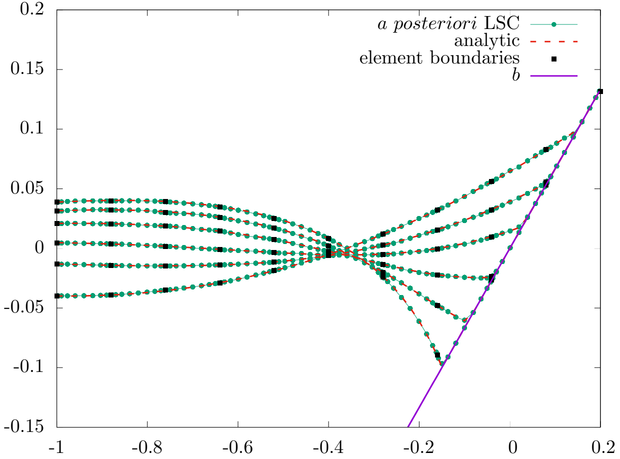

FIGURE – Test 5 - Carrier and Greenspan's periodic solution - Free surface elevation computed for different values of time in the range $[14.5T, 15T]$ for $k = 8$ and $n_e = 10$.

Carrier and Greenspan transient

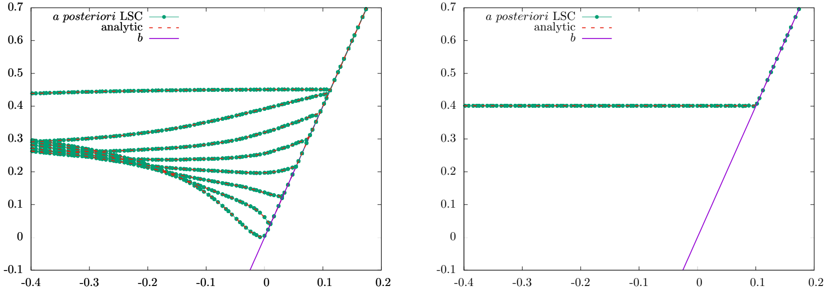

FIGURE – Test 4 - Carrier and Greenspan's transient solution - Free surface elevation for different values of time in the range [0.5 s, 23 s] (left) and at t = 200 s (right) for k = 3 and n e = 50.

Carrier and Greenspan transient

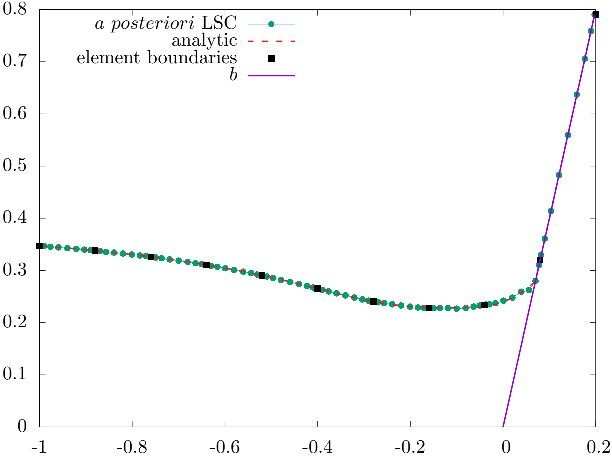

FIGURE – Test 4 - Carrier and Greenspan's transient solution, for k = 8 and n e = 10

Conclusion

- New subcell DG-FV formulation for nonlinear Shallow water equation
- The resulting algorithm accurately handles strong shocks with no robustness issues
- It ensures the preservation of the water height positivity at the subcell level
- It preserves the class of motionless steady states (well-balancing)
- It retains the highly accurate subcell resolution of DG schemes
- The procedure is furthermore totally parameter free

Future works

- Investigate moving mesh case, based on an Arbitrary-Lagrangian-Eulerian ALE (in progress)
- Coupling with a floating object.
- Extend to a general 2D case

References I

A. Haidar et al.
A posteriori finite-volume local subcell correction of high-order discontinuous galerkin formulations for the nonlinear shallow-water equations.
J. Comput. Phys., 2021.
Article submitted.

F. Vilar.
A posteriori correction of high-order discontinuous galerkin scheme through subcell finite volume formulation and flux reconstruction.
J. Comput. Phys., 387 :245–279, 2019.